Supporting Information

Redox-active polyoxometalate-based crystalline materials-immobilized noble metal nanoparticles: spontaneous reduction and synergistic catalytic activity

Dong-Ying Du, Jun-Sheng Qin, Chun-Gang Wang, Xian-Chun Liu, Shun-Li Li, Zhong-Min Su,* Xin-Long Wang, Ya-Qian Lan* and En-Bo Wang

Institute of Functional Material Chemistry, Key Lab of Polyoxometalate Science of Ministry of Education, Faculty of Chemistry, Northeast Normal University, Changchun 130024 (P. R. China). E-mail: zmsu@nenu.edu.cn; lanyq176@nenu.edu.cn

S1 Materials and measurements

All the chemicals were obtained from commercial sources, and were used without further purification. Deionized water was used for all experiments. Mo, Mn and P were determined with ICP-OES Spectrometer (USA). IR spectrum was performed in the range 4000–400 cm^{-1} using KBr pellets on an Alpha Centaurt FT/IR spectrophotometer. The X-ray powder diffraction (XRPD) data were recorded on a Bruker D8 Advance diffractometer. UV/Vis spectroscopy was performed with a Varian Cary 50 spectrophotometer in the range of 250–800 nm. XPS analysis was performed on a thermo ECSALAB 250 spectrometer with an Al Kα (1486.6 eV) achromatic X-ray source. The XPS binding energy (BE) was internally referenced to the aliphatic C(1s) peak (BE, 284.6 eV).

S2 Single-crystal X-ray diffraction

Suitable single crystal of **IFMC-101** was selected and mounted onto the end of a thin glass fiber using Fomblin oil. Single crystal X-ray diffraction data for **IFMC-101** were recorded on a Bruker APEXII CCD diffractometer with graphite-monochromated Mo Kα radiation (λ = 0.71069 Å) at 293 K. Absorption corrections were applied using multi-scan technique. The structure was solved by Direct Method of SHELXS-97[1] and refined by full-matrix least-squares techniques using the SHELXL-97 program[2] within WINGX.[3] Those hydrogen atoms attached to lattice water molecules were not located.

S3 Characterization of metal nanoparticles

Field-emission scanning electron microscopy (FE SEM) images were obtained with a XL30 ESEM FEG microscope equipped with energy dispersive X-ray spectroscopy (EDS). Transmission electron microscopy (TEM) with EDS examination of the samples were performed using a TECNAI F20 microscope. The samples were prepared by placing microdrops of colloid solution on a holey carbon copper grid. The subsequent analysis for the size distribution of the particles was based on the counting of ca. 200 particles.

S4 Catalytic reduction of 4-nitrophenol (4-NPh)

The reduction of 4-NPh by $NaBH_4$ was chosen as a model reaction to test the catalytic activity of **Au@IFMC-101**. Generally, the reaction proceeded under ambient conditions. The 4-NPh solution exhibited a strong absorption peak at 317 nm in neutral or acidic conditions. Upon the addition of freshly prepared and ice-cold $NaBH_4$ solution, the absorption peak of 4-NPh changed from 317 to 400 nm immediately, corresponding to the color change of light yellow to yellow-green due to the formation of 4-nitrophenolate ion. To a mixture of 2.3 mg of $NaBH_4$ dispersed in 1 mL ice-sold

distilled water, 1 mL of 0.12×10^{-3} mol·L^{-1} 4-NPh was added. To this solution, 22 mg of catalyst (**Au@IFMC-101**) was added. After **Au@IFMC-101** was added, the characteristic absorption peak of 4-nitrophenolate ion at 400 nm gradually decreased, while a new peak at ~300 nm, ascribed to 4-APh, appeared. The peak of the 4-nitrophenolate ions diminished after 8 min. The absorption spectra of the solution were measured in the range of 250-800 nm. The rate constants of the reduction process were determined through monitoring the change in absorbance at 400 nm as a function of time.

To make a comparison, the activity of **IFMC-101** was also carried out under similar conditions. The result suggests that **IFMC-101** can catalyze this reaction with obvious longer reaction time than that of **Au@IFMC-101**.

S5 Crystal data and structure refinement for IFMC-101 (Table S1)

	IFMC-101
Empirical formula	$H_{86}Mn_{10}Mo_{24}Na_6O_{158.5}P_{17}$
*F*w	6139.08
Crystal system	Tetragonal
Space group	$I4_1/acd$
a (Å)	27.0880(13)
b (Å)	27.0880(13)
c (Å)	41.2550(14)
V (Å^3)	30271(2)
Z	8
D_c (Mg·m^{-3})	2.694
Abs.coeff.(mm^{-1})	3.041
θ range (deg)	1.45 – 28.27
F(000)	23464
reflns collected	88182
Independent reflns	9272
GOF on F^2	1.075
R_{int}	0.0459
R_1 [I>2σ][a]	0.0451
wR_2 (all data)[b]	0.1393
Largest residuals [e Å^{-3}]	2.143/-1.493

[a] $R_1 = \Sigma||F_o| - |F_c||/\Sigma|F_o|$. [b] $wR_2 = |\Sigma w(|F_o|^2 - |F_c|^2)|/\Sigma|w(F_o^2)^2|^{1/2}$.

S6 Figures in Supporting Information

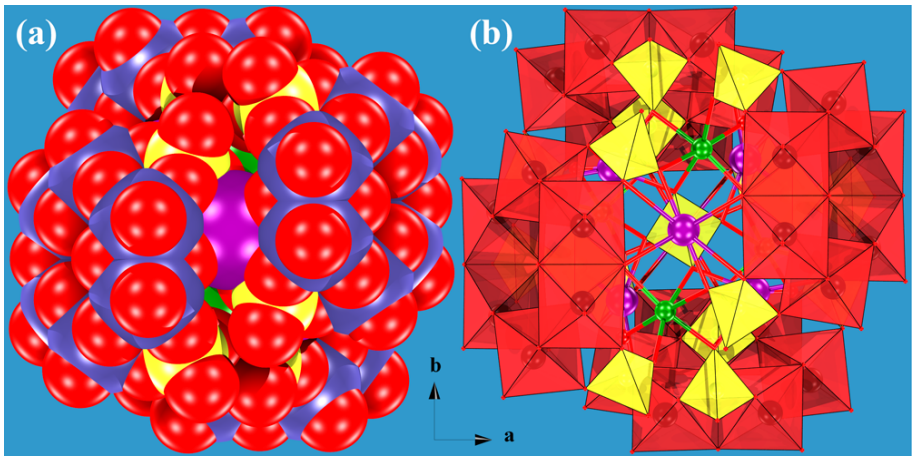

Fig. S1 The Spacefill and Polyhedral representations of tetrameric cluster $\{[Na_6Mn_4(PO_4)(H_2O)_4]\subset[P_4Mo_6O_{31}H_6]_4\}^{13-}$ in **IFMC-101**.

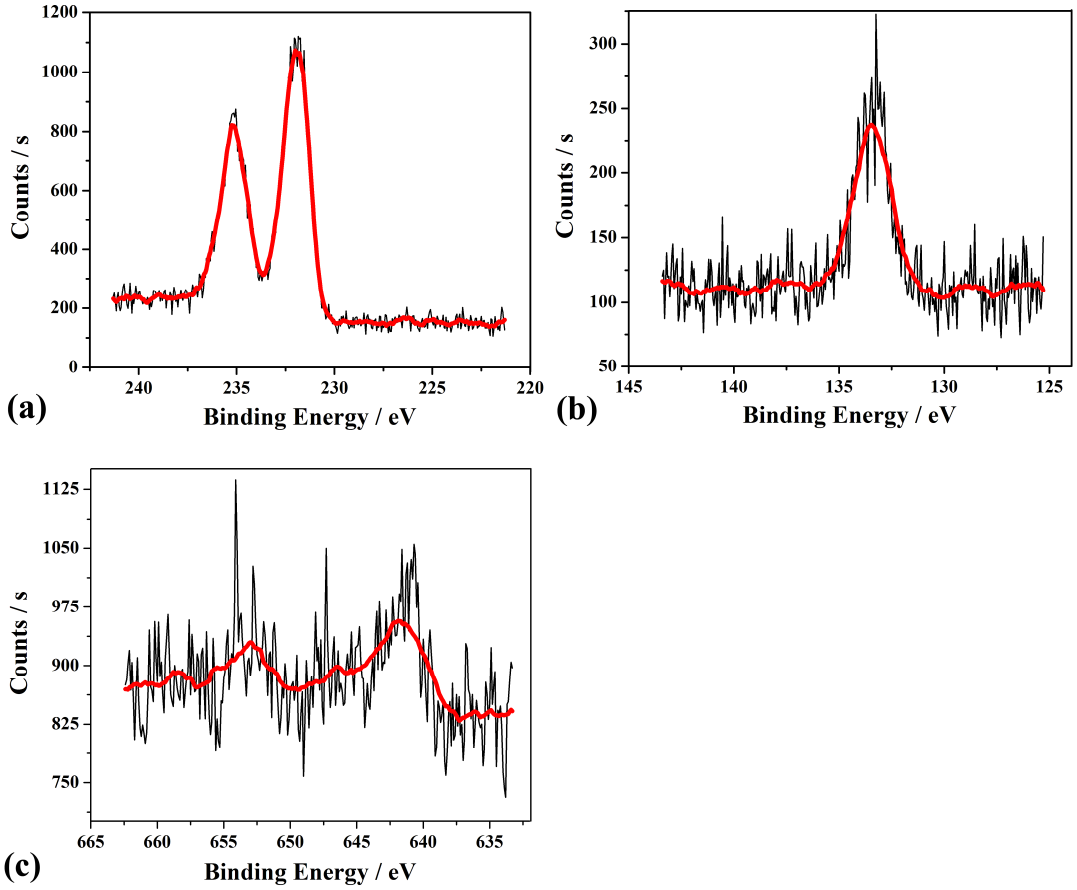

Fig. S2 The XPS results of Mo (a), P (b) and Mn (c) for **IFMC-101**, respectively.

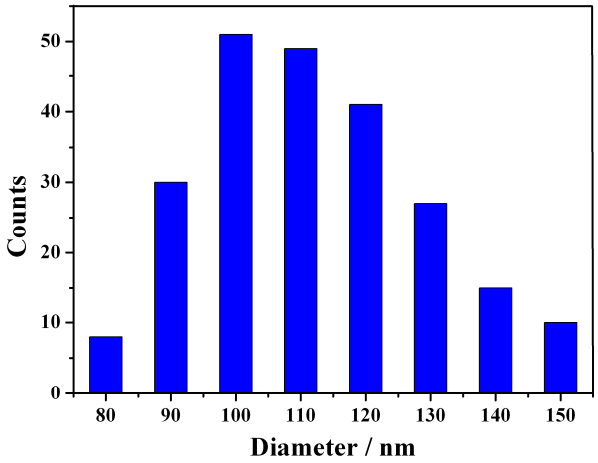

Fig. S3 The Au NPs size distribution of **Au@IFMC-101** prepared by the first method.

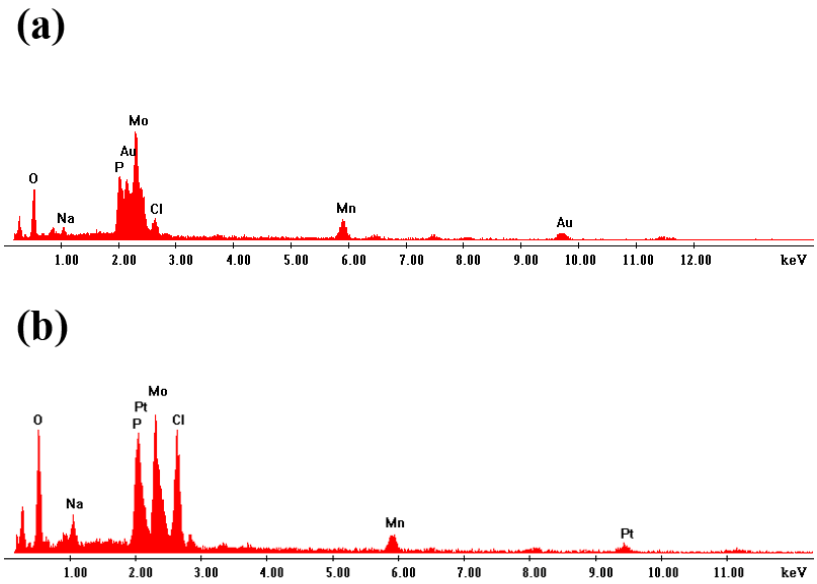

Fig. S4 EDS data for **Au@IFMC-101** (a) and **Pt@IFMC-101** (b) samples prepared by the first method, respectively.

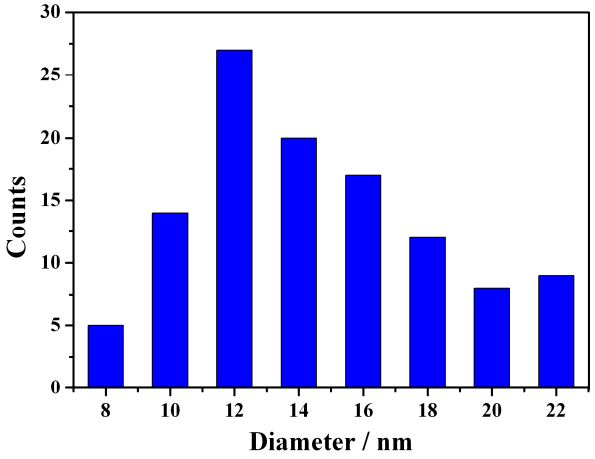

Fig. S5 The Au NPs size distribution of **Au@IFMC-101** prepared by the second method.

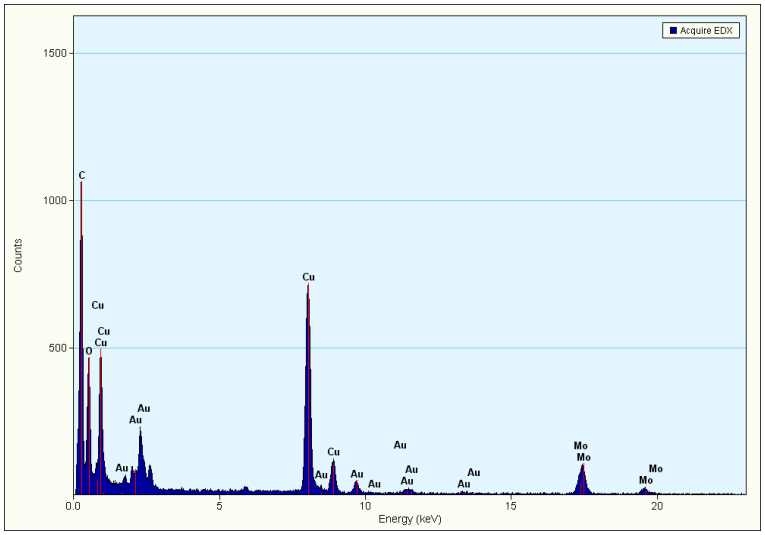

Fig. S6 EDS data for **Au@IFMC-101** sample prepared by the second method.

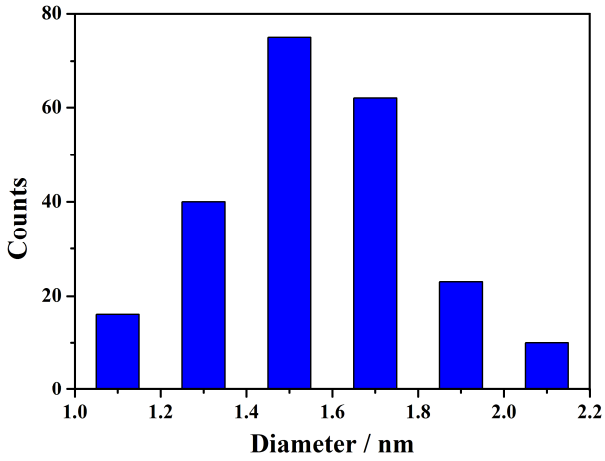

Fig. S7 The Pt NPs size distribution of **Pt@IFMC-101** prepared by the second method.

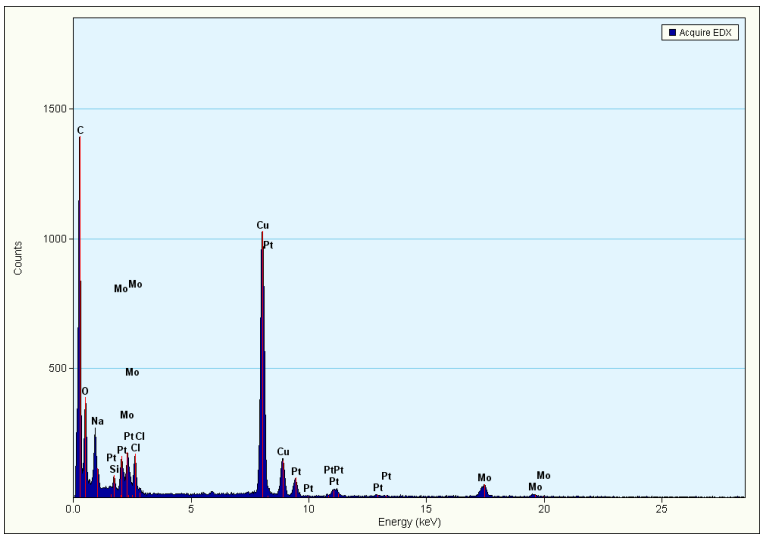

Fig. S8 EDS data for **Pt@IFMC-101** sample prepared by the second method.

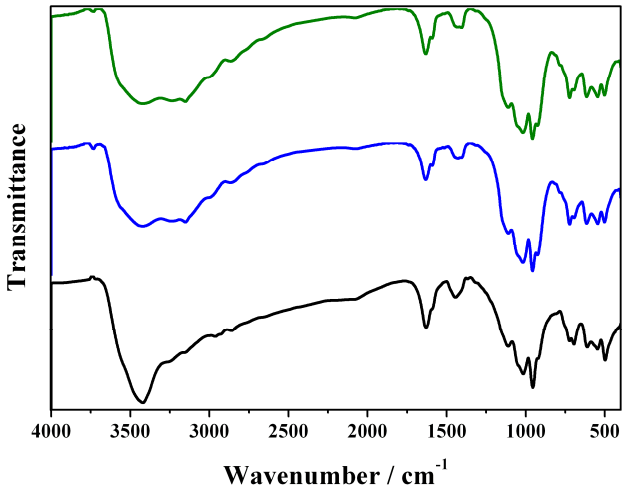

Fig. S9 The IR curves of **IFMC-101** after different treatment: the as-synthesized samples (*black*), the as-synthesized samples after reduction of $HAuCl_4$ (*blue*), and the as-synthesized samples after reduction of $PtCl_4$ (*green*).

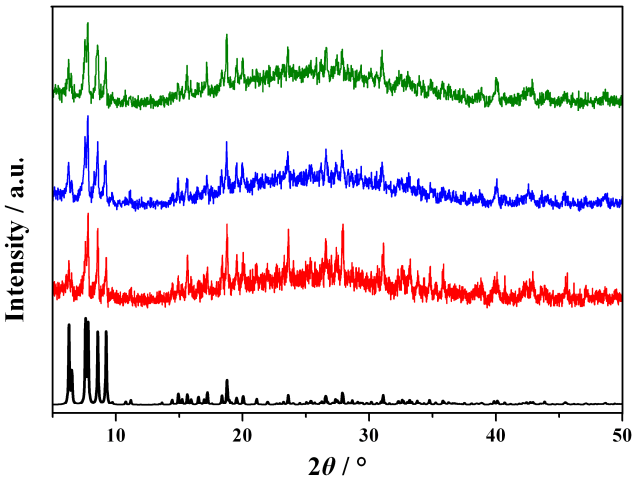

Fig. S10 The XRPD patterns of **IFMC-101**: the stimulated pattern (*black*), the as-synthesized samples (*red*), the as-synthesized samples after reduction of $HAuCl_4$ (*blue*) and the as-synthesized samples after reduction of $PtCl_4$ (*green*).

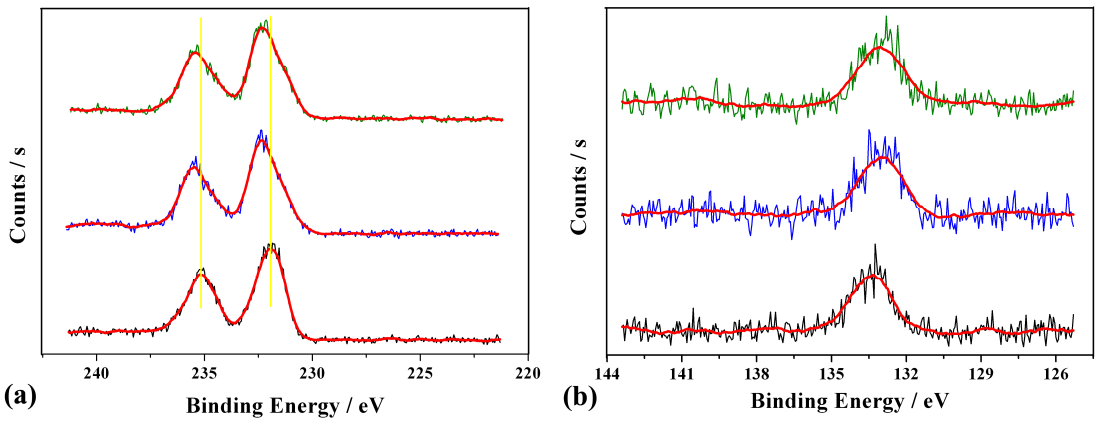

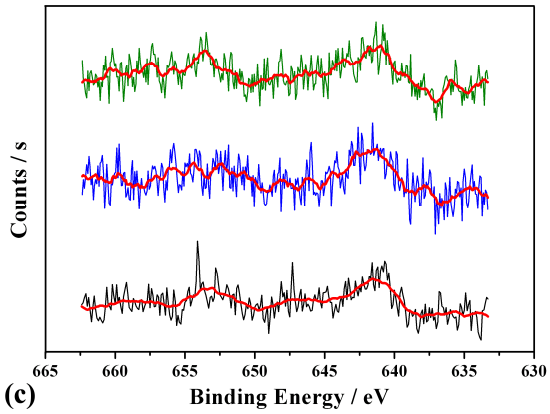

Fig. S11 The XPS analysis for Mo (a), P (b), Mn (c) in **IFMC-101**, in which the as-synthesized samples (*black*); the as-synthesized samples after reduction of $HAuCl_4$ (*blue*); and the as-synthesized samples after reduction of $PtCl_4$ (*green*).

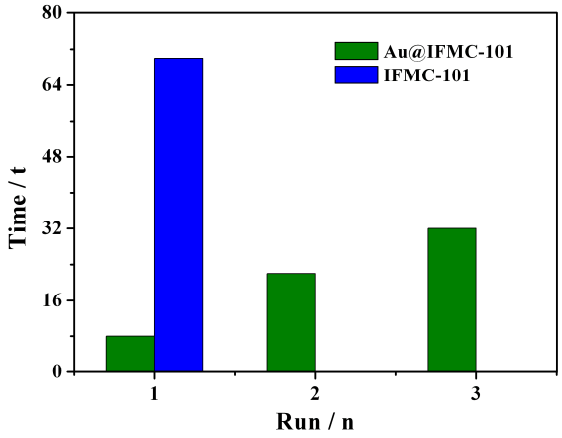

Fig. S12 The reaction time of catalytic reduction of 4-NPh in the presence of **Au@IFMC-101** and **IFMC-101**, respectively.

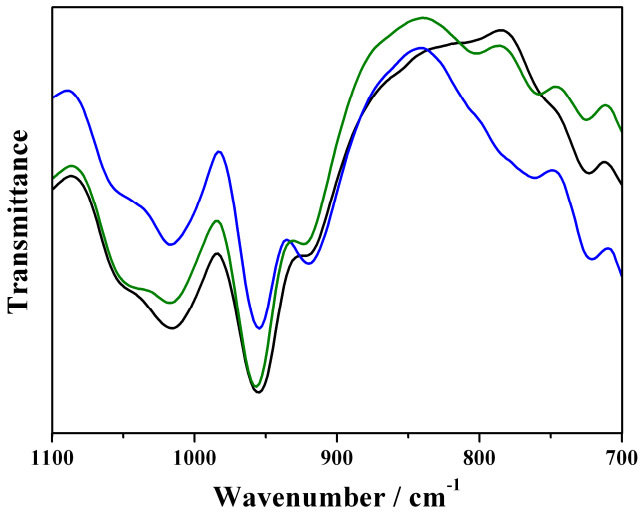

Fig. S13 The IR spectra of **IFMC-101** (*black*), and **Au@IFMC-101** (*blue*) and **IFMC-101** (*green*) after the catalytic reduction of 4-NPh, respectively.

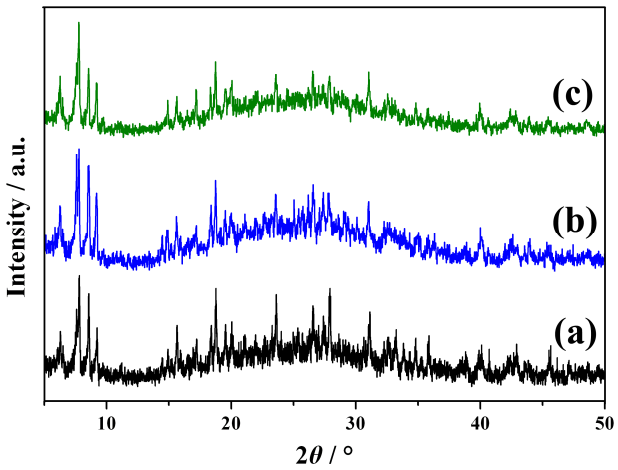

Fig. S14 The XRPD patterns of **IFMC-101** (a), and the XRPD patterns of **Au@IFMC-101** (b) and **IFMC-101** (c) after the catalytic reduction of 4-NPh, respectively.

Reference

1 G. M. Sheldrick, SHELXS-97, Programs for X-ray Crystal Structure Solution, University of Göttingen: Göttingen, Germany, **1997**.

2 G. M. Sheldrick, SHELXL-97, Programs for X-ray Crystal Structure Refinement, University of Göttingen: Göttingen, Germany, **1997**.

3 L. J. Farrugia, WINGX, A Windows Program for Crystal Structure Analysis; University of Glasgow; Glasgow, UK, **1988**.